PeptiCHIP: a novel microfluidic-based chip platform for tumour antigen landscape identification

Sara Feola
University of Helsinki https://orcid.org/0000-0002-4012-4310
Markus Haapala
University of Helsinki
Karita Peltonen
University of Helsinki
Cristian Capasso
University of Helsinki
Beatriz Martins
University of Helsinki
Gabriella Antignani
University of Helsinki
Antonio Federico
University of Tampere
Vilja Pietiäinen
Institute for Molecular Medicine Finland FIMM
Jacopo Chiaro
University of Helsinki
Michaela Feodoroff
University of Helsinki
Antti Rannikko
Department of Urology University of Helsinki
Manlio Fusciello
University of Helsinki
Satu Koskela
Research & Development Finnish Red Cross Blood Service Helsinki
Jukka Partanen
Research & Development Finnish Red Cross Blood Service
Firas Hamdan
University of Helsinki
Sari Tähkä
University of Helsinki
Erkko Ylösmäki

University of Helsinki https://orcid.org/0000-0001-9678-2614
Dario Greco
Tampere University https://orcid.org/0000-0001-9195-9003
Mikaela Grönholm
University of Helsinki
Tuija Kekarainen
Kuopio Center for Gene and Cell Therapy
Masoumeh Eshaghi
Kuopio Center for Gene and Cell Therapy
Olga L. Gurvich
Kuopio Center for Gene and Cell Therapy
Seppo Ylä-Herttuala
University of Eastern Finland https://orcid.org/0000-0001-7593-2708
Rui Mamede Branca
Karolinska Institutet https://orcid.org/0000-0003-3890-6476
Janne Lehtiö
Karolinska Institutet https://orcid.org/0000-0002-8100-9562
Tiina Sikanen
University of Helsinki
Vincenzo Cerullo (✉ vincenzo.cerullo@helsinki.fi)
University of Helsinki

Article

Keywords: Ligandome, HLA peptides, affinity purification, microfluidics, thiol-enes

Posted Date: March 3rd, 2021

DOI: https://doi.org/10.21203/rs.3.rs-156531/v1

Abstract

Identification of HLA class I ligands from the tumour surface (ligandome or immunopeptidome) is essential for designing T-cell mediated cancer therapeutic approaches. However, the sensitivity of the process for isolating MHC-I restricted tumor-specific peptides has been the major limiting factor for reliable tumor antigen characterization, making clear the need for technical improvement. Here, we describe our work from the fabrication and development of a novel microfluidic-based chip (PeptiCHIP) and to its use to identify and characterize tumor-speficic ligands on clinically relevant human organoids. Specifically, we assessed the potential of immobilizing a pan-HLA antibody on solid surfaces via well-characterized streptavidin-biotin chemistry, overcoming the limitations of the cross-linking chemistry used to prepare the affinity matrix with the desired antibodies in the immunopeptidomics workflow. Furthermore, to address the restrictions related to the handling and the limited availability of tumour samples, we further developed the concept towards the implementation of a microfluidic through-flow system. Thus, the biotinylated pan-HLA antibody was immobilized on streptavidin-functionalized surfaces, and immune-affinity purification (IP) was carried out on customized microfluidic pillar arrays made of thiol-ene polymer. Compared to the standard methods reported in the field, our methodology drastically reduces the handling, the amount of antibody and the time required for peptide isolation. In this work, we carefully examined the specificity and robustness of our customized technology for immunopeptidomics workflows. We tested this novel platform by immunopurifying HLA-I complexes from as few as 106 cells both in a widely studied B-cell line and in patients-derived ex vivo cell cultures. After the final elution in mild acid, HLA-I-presented peptides were identified by tandem mass spectrometry and further investigated by in vitro methods. These results highlight the potential to exploit microfluidics-based strategies in immunopeptidomics platforms and in personalized immunopeptidome analysis from cells isolated from individual tumour biopsies to design tailored cancer therapeutic vaccines.

Introduction

Cancer immunotherapy relies on the priming of T cells, the generation and stimulation of cytotoxic CD8 T lymphocytes (CTLs) within the tumour microenvironment (TME), and the establishment of an efficient and durable anti-tumour immune response (1). In this context, the breakthrough of immune-checkpoint inhibitors to release the brakes on the immune system clearly showed the need to identify immunogenic T-cell epitopes to use for personalized therapeutic cancer vaccines (2). Currently, the direct isolation of the entire HLA-presented peptide pool is the only reliable approach to identify the naturally presented HLA-I landscape in human cell lines (3, 4), tumour tissues (5-7) and bodily fluids such as plasma (8). This methodology is based on immunoaffinity purification (IP) of HLA-I complexes from mild detergent-solubilized lysates, followed by extraction of HLA-I peptides. Then, the peptides are separated by chromatography and directly injected into a mass spectrometer (MS). Currently, several techniques originating from an immunoaffinity purification approach are suitable for immunopeptidomics analysis (9, 10). Indeed, significant technological advances in chromatography, MS and bioinformatics tools have

facilitated the analysis of thousands of HLA-I peptides and enabled a greater understanding of the dynamic nature of the entire HLA-I landscape in tumour cells.

Nevertheless, in the last 20 years, few improvements related to the sensitivity of the state-of-the-art methodologies have been reported in the entire immunopeptidomics pipeline, making this step the Achilles heel in the whole antigen discovery workflow (11). Indeed, the limited size/amount of clinically relevant samples (e.g., tissue needle biopsies) challenges the IP efficiency and frequently strains the limits of detection at the Mass Spectrometry level. Therefore, the pooling of several samples is often required, making analysis of samples from a single individual very challenging (12). However, there can be remarkable inter-patient variation in the HLA profiles of patients with similarly diagnosed cancer, and this is lost in traditional IP of complexes. In addition, several studies reported that IP technology is the origin of significant peptide loss during sample preparation (13) (14). A key to achieve a comprehensive HLA peptide profiling is the development of the entire workflow including the pre-analytical process prior LC-MS-analysis; an increased sensitivity in the methodology requires standardized protocols, comparable results between different laboratories and standardized controls (13). Here, for the first time, we sought to establish and characterize a microfluidics-based immobilization strategy for IP of the HLA-antigen landscape for MS-based immunopeptidomics analysis that is suitable for both basic and translational studies. Specifically, we carried out the entire workflow in a single thiol-ene polymer-based microfluidic chip incorporating streptavidin-functionalized micropillars for immobilization of a biotinylated anti-pan-HLA antibody. The described protocol (including microchip fabrication and functionalization) requires one day instead of 3-5 days, as reported for the currently used methodologies for the antigen landscape investigation, making our novel technology faster than the traditional methods in the field.

Moreover, the cost of ligandome investigation with the conventional IP methodology is significantly high as a result of the great consumption of the affinity matrix which requires in-house production of a relatively large amount of monoclonal antibodies from hybdridoma cells (13). For the first time, our approach integrates a miniaturized sample preparation system into immunopeptidomics analysis, leading to low reagent consumption, hence reducing the use of these expensive reagents as well. Both of these advantages, fast speed (< 24 h) and miniaturization also enable the processing of cancer patient tissue samples/*ex vivo* cell cultures, opening novel revenues for personalized T-cell therapies in precision cancer medicine.

In our work, we exploited the thiol-ene polymer based micropillar chip to implement the immunopeptidomics workflow, carefully analysing the robustness of our technology and further validating it through relevant *in vitro* assays.

Material And Methods

Cell line and reagents

The EBV-transformed human lymphoblastoid B-cell line JY (ECACC HLA-type collection, Sigma Aldrich) was cultured in RPMI 1640 (GIBCO, Invitrogen, Carlsbad, CA, USA) supplemented with 1% GlutaMAX

(GIBCO, Invitrogen, Carlsbad, CA, USA) and 10% heat inactivated foetal bovine serum (HI-FBS, GIBCO, Invitrogen, Carlsbad, CA, USA).

Streptavidin (*Streptomyces avidinii*, affinity purified, lyophilized from 10 mm potassium phosphate, ≥13 U/mg protein) was purchased from Sigma-Aldrich (Saint Louis, Missouri, USA).

Biotin-conjugated anti-human HLA-A, B, C clone w6/32 was purchased from Biolegend (San Diego, CA, USA) for analysis.

The following peptides were purchased from Ontores Biotechnologies Co., Ltd., were used throughout the study: KVLEYVIKV (gene name MAGE A1), ILDKKVEKV (gene name HSP90), and QLVDIIEKV (gene name PSME3).

Additionally, the following peptides were purchased from Chempeptide (Shangai, China):

VIMDALKSSY (gene name NNMT), FLAEGGGVR (gene name FGA) and EVAQPGPSNR (gene name HSPG2).

Ovarian tumour biopsy and ethical consideration

The ovarian tumour biopsy was collected from a patient with ovarian metastatic tumour (high grade serous), who signed an informed consent, under the studies approved by the Research Ethics Committee of the Northern Savo Hospital District with the approval number 350/2020. The samples were chopped in small pieces and treated with a digestion buffer containing collagenase type D (Roche) 1mg/ml, Hyaluronidase (Sigma Aldrich) 100 mg/ml and DNase I (Roche) 1mg/ml for 1h at 37°C. The cell suspension was sequentially passed through a 500 mm and 300 mm cell strainer (pluriSelect) to obtain single cells.

Renal cell carcinoma and bladder tumour samples and ethical considerations

Patient tissue samples for organoid cultures were obtained from the DEDUCER study (Development of Diagnostics and Treatment of Urological Cancers) at Helsinki University Central Hospital with approval number HUS/71/2017, 26.04.2017, ethical committee approval number 15.03.2017 Dnro 154/13/03/02/2016, and patient consent. The kidney sample was obtained from a nephrectomy of an adult male with a clear cell renal cell carcinoma (ccRCC, pTNM stage pT3a G2). The benign kidney tissue sample was used for the experiments. The carcinoma urothelial (bladder cancer, high grade, gradus III, 1x1 cm) was obtained from adult female, and the cancer tissue sample was used for the organoid culture.

Clear cell renal carcinoma and bladder tumour organoid culture

Cells were isolated from the original tissue instantly after surgery by dissociating the tissue into small pieces and treating it with collagenase (40 units/ml) for 2–4 h. Benign and cancer cells of the kidney of a clear cell renal cell carcinoma patient cells were grown as organoids in F-medium [3:1 (v/v) of F-12

nutrient mixture (Ham) - DMEM (Invitrogen), 5% FBS, 8.4 ng/mL cholera toxin (Sigma), 0.4 µg/mL hydrocortisone (Sigma), 10 ng/mL epidermal growth factor (Corning), 24 µg/mL adenine (Sigma), 5 µg/mL insulin (Sigma), 10 µM ROCK inhibitor (Y-27632, Enzo Life Sciences, Lausen, Switzerland) and 1% penicillin-streptomycin with 10% Matrigel (Corning). The bladder tumour-derived organoids were grown in hepatocyte calcium medium (Corning)(15) supplemented with 5% CSFBS (Thermo Fisher Scientific), 10 µM Y-27632 RHO inhibitor (Sigma), 10 ng/mL epidermal growth factor (Corning), 1% GlutaMAX (Gibco), 1% penicillin-streptomycin and 10% Matrigel. $6x10^6$ cells were collected by centrifugation, washed in PBS to remove Matrigel and snap frozen before analyses.

HLA typing

The clinical HLA typing of tumour samples (ccRCC and bladder) was performed by the European Federation for Immunogenetics (EFI) -accredited HLA laboratory of the Finnish Red Cross Blood Service. Allele determination of three classical HLA-I genes HLA-A, -B and -C was performed by targeted PCR based next generation sequence (NGS) technique according to the protocol provided by the manufacturer (NGSgo® Workflow, GenDx, Utrecht, The Netherlands).

The allele assignment at 4-field resolution level was implemented by NGSengine Version: 2.11.0.11444 (GenDx, Utrecht, The Netherlands) using IPD IMGT/HLA database Release 3.33.0, https://www.ebi.ac.uk/ipd/imgt/hla/.

Flow cytometry analysis

The following antibodies were used to analyse the cell surface expression of HLA-A2 and HLA-A, B, and C: PE-conjugated anti-human HLA-A2 (clone BB7.2, BioLegend 343306 San Diego, CA, USA), PE-conjugated anti-human HLA-A, B, and C (clone W6/32, BioLegend 311406, San Diego, CA, USA), and Human TruStain FcX block (BioLegend B247182, San Diego, CA, USA).

The data were acquired using a BDLSR Fortessa Flow Cytometer. Flow cytometric analysis of renal cell carcinoma and bladder tumour-derived organoids was performed using a BD Accuri 6 plus (BD Biosciences) and analysed with FlowJo software (Tree Star, Ashland, OR, USA).

Immobilized biotinylated pan-HLA antibody titer assay

The amount of immobilized biotinylated pan-HLA antibody has been tittered comparing the amount of the antibody in the feed solution versus the output solution. In detail, 12.5mg of anti-panHLA (Biolegend, cat. 311434, clone W6/32, biotin conjugated) in 25ml was added into microchip at each cycle and incubated for 15 minutes at room temperature. After the incubation time, the microchip was washed three times with 200mL of PBS and the elute collected. The antibody in the output solution was then quantified by ELISA. Briefly, maxisorb ELISA Nunc plates were coated with the output solution overnight at +4°C. After washing, 4%BSA (BioTop Oy) in PBS was added and incubated for 2h at 37°C, followed by washing steps in 0.05%Tween20 (Sigma Aldrich). Streptavidin/HRP (Pierce) was added for 30 minutes, followed

by additional washing steps. Finally, TMB (Pierce) solution was applied for 20 minutes and Sulfuric Acid (Sigma Aldrich) 0.16M was used to stop the reaction and the plate read at 450 nm. The amount of biotinylated pan-HLA antibody was quantified by extrapolating the signal into a linear range (signal vs concentration) of a standard curve.

Purification and concentration of HLA class I peptides

HLA class I peptides were immunoaffinity purified from the JY human cell line using biotin-conjugated anti-human HLA-A, B, and C antibodies (clone W6/32, BioLegend 311434 San Diego, CA, USA). For sample preparation, the snap-frozen cell pellet was pipetted up and down 20 times in lysis buffer. The lysis buffer contained 150 mM NaCl, 50 mM TRIS-HCl, pH 7.4, protease inhibitors (A32955 Thermo Scientific Pierce, Waltham, Massachusetts, USA) and 1% Igepal (I8896 Sigma Aldrich, St. Louis, Missouri, USA). The lysates were first cleared by slow centrifugation for 10 min at 500xg, and then the supernatant was centrifuged for 30 min at 25,000xg. Next, HLA-I complexes were immunoaffinity purified from the cleared lysate with anti-human HLA-A, HLA-B, and HLA-C biotin-streptavidin bound to the micropillars of the biotinylated thiol-ene CHIP. The CHIPs were first washed three times with PBS, and then the HLA molecules were eluted at room temperature by adding acetic acid 7% (A113 Fisher Scientific, Leicestershire UK) in 50% MetOH (10402824 Fisher Scientific, Leicestershire UK).

Eluted HLA peptides and the subunits of the HLA complexes were desalted using SepPac-C18 cartridges (Waters) according to the protocol previously described by Bassani et al. (16). Briefly, the cartridge was prewashed with 80% acetonitrile in 0.1% trifluoroacetic acid (TFA) and then with 0.1% TFA. The peptides were purified from the HLA-I complex by elution with 30% acetonitrile in 0.1% TFA. Finally, the samples were dried using vacuum centrifugation (Eppendorf).

LC-MS/MS analysis of HLA class I peptides

Each dry sample was dissolved in 10 µL of LCMS solvent A (0.1% formic acid). The nanoElute LC system (Bruker, Bremen, Germany) injected and loaded the 10 µl of sample directly onto the analytical column (Aurora C18, 25 cm long, 75 µm ID, 1.6 µm bead size, Ionopticks, Melbourne, Australia) constantly kept at 50°C by a heating oven (PRSO-V2 oven, Sonation, Biberach, Germany). After washing and loading sample at a constant pressure of 800 bar, the LC system started a 30 min gradient from 0 to 32% solvent B (acetonitrile, 0.1% formic acid), followed by increase to 95% B in 5 min, and finally a wash of 10 min at 95% B, all at a flow rate of 300 nL/min. Online LC-MS was performed using a Tims TOF Pro mass spectrometer (Bruker, Bremen, Germany) with the CaptiveSpray source, capillary voltage 1500V, dry gas flow of 3L/min, dry gas temperature at 180°C. MS data reduction was enabled. Mass Spectra peak detection maximum intensity was set to 10. Mobilogram peak detection intensity threshold was set to 5000. Mass range was 300-1100 m/z, and mobility range was 0.6-1.30 V.s/cm^2. MS/MS was used with 3 PASEF (Parallel Accumulation – Serial Fragmentation) scans (300ms each) per cycle with a target intensity of 20000 and intensity threshold of 1000, considering charge states 0-5. Active exclusion was used with release after 0.4 min, reconsidering precursor if current intensity is >4 fold the previous

intensity, and a mass width of 0.015 m/z and a 1/k0 width of 0.015 V.s/cm^2. Isolation width was defined as 2.00 m/z for mass 700 m/z and 3.00 m/z for mass 800 m/z. Collision energy was set as 10.62 eV for 1/k0 0.60 V.s/cm^2 and 51.46 eV for 1/k0 1.30 V.s/cm^2. Precursor ions were selected using 1 MS repetition and a cycle overlap of 1 with the default intensities/repetitions schedule.

Proteomics database search

All MS/MS spectra were searched by PEAKS Studio X+ (v10.5 build 20191016) using a target-decoy strategy. The database used was the Swissprot Human protein database (including isoforms, 42373 entries, downloaded from uniprot.org on 20191126).

A precursor mass tolerance of 20 ppm and a product mass tolerance of 0.02 Da for CID-ITMS2 were used. Enzyme was none, digest mode unspecific, and oxidation of methionine was used as variable modification, with max 3 oxidations per peptide. A false discovery rate (FDR) cut-off of 1% was employed at the peptide level. The mass spectrometry proteomics data have been deposited to the ProteomeXchange Consortium via the PRIDE partner repository with the dataset identifier PXD022194. The dataset is currently hidden but will be made public upon eventual acceptance of the current manuscript.

Algorithms used for prediction of peptide ligands

Affinity to the corresponding HLA alleles was predicted for all eluted peptides identified in the JY cell line using NetMHC4.0. The threshold for binding was set to rank 0.5% to include only the strong binding partners.

GIBBS clustering analysis

Clustering of peptides into groups based on sequence similarities was performed using the GibbsCluster-2.0 tool with the default setting.

PBMC stimulation protocol

PBMCs from healthy donors were either purchased from Immunospot (Bonn, Germany) or isolated from whole blood of healthy donors using a Ficoll (Merck Millipore) density gradient and cultured in RPMI-1640 supplemented with 10% FBS (Gibco), 1% penicillin-streptomycin (Gibco), 1% GlutaMAX (Gibco), 15 mM HEPES, 50 µM b-mercaptoethanol (Gibco), and 1 mM sodium pyruvate (Gibco). The PBMCs were cultured and stimulated according to the following schedule:

- Day 0: thawing of the PBMCs and addition of 10 ng/mL IL-4, 800 IU/mL GM-CSF, 10 ng/mL IL-7 and 5 ng/mL IL-15.
- Day 2: addition of 10 ng/ml LPS, 50 IU/ml IFN-γ, 10 ng/ml IL-4, 800 IU/ml GM-CSF, 60 ng/ml IL-21, and 5 mg/ml peptides.
- Day 5 and 7: addition of 5 ng/ml IL-15, 5 ng/ml IL-7, 60 ng/ml IL-21, and 5 mg/ml peptides.

- Day 9: addition of 5 ng/ml IL-15, 5 ng/ml IL-7, and 5 mg/ml peptides.

PBMCs from patients were stimulated as previously described (17) with slightly modifications. $0.2x10^6$ cells were allocated per well and cultured in RPMI-1640 (GIBCO, Invitrogen, Carlsbad, CA, USA) supplemented with 20%FBS (HI GIBCO, Invitrogen, Carlsbad, CA, USA), 1% penicillin-streptomycin (GIBCO, Invitrogen, Carlsbad, CA, USA), 1% GlutaMAX (GIBCO, Invitrogen, Carlsbad, CA, USA) and in presence of IL-4 (Biotechne) and GM-CSF (Biotechne) for 24h. 1 µM Peptide (Chempeptide), 0.5 ng/ml IL-7 (Biotechne) and 20 mg/ml Poly-I:C (Invitrogen) were added after 24 h. The stimulation lasted 9 days.

$CD8^+$ T cell isolation

$CD8^+$ T cells were isolated by MACS depletion (Miltenyi Biotec, Bergisch Gladbach, Germany) from PBMCs stimulated according to the aforementioned protocol.

Real-time impedance-based cytotoxicity assay

The cytotoxicity assay was performed using the xCELLigence real-time cell analysis system (ACEA Biosciences Inc.). Briefly, 80,000 JY cells or 75,000 ccRCC cells were seeded in a total volume of 50 ml per well (in an antiCD19 pre-coated 8-well plate in case of the JY) and cultured for 24 h at 37°C in 5% CO_2. After 24 h, the effector cells (purified CD8 T cells) were added at a target (E/T) ratio of 1:1. The effector and target cells were cocultured for 36 h, and the CI of the target cells was measured every 1 h. The normalized cell index (NCI) was used for the analysis, and the following formula was applied:

% Specific Cytolysis at time t = 1- NCI(s)t/ NCI(M)t

where NCI is the normalized cell index, s is the Sample and M is Mock Effector Control.

Microchip design, fabrication and functionalization

The microchips used in this work incorporated a 30´4´0.2 mm^3 (length´width´height) microchannel featuring an array of ca. 14 400 micropillars (diameter 50 µm, interpillar distance 100 mm from centre to centre) in a hexagonal lattice (Fig. 1). The internal volume of the microchannel was ca. 25 µL. The microchips were made of off-stoichiometric thiol-enes (OSTE) polymer composition as previously described by Tähkä et al. (17) and functionalized with biotin prior to use. Briefly, the OSTE prepolymer was prepared mixing a tetrafunctional thiol (pentaerythritol tetrakis(3-mercaptopropionate), Thiocure® PETMP, Bruno Bock, Marschacht, Germany) and a trifunctional 'ene' (triallyl-1,3,5-triazine-2,4,6(1H,3H,5H)-trione, 98%, Sigma Aldrich, St. Louis, MO) monomers at a ratio that yielded a 50% molar excess of thiol functional groups (i.e., 12.5% molar excess of the tetrathiol monomer) in the bulk solution. The monomer mixture was then poured onto a premade polydimethylsiloxane (Sylgard 184, Down Corning Corporation, Midland, MI) mould, incorporating a negative replica of the micropillar array, and kept under vacuum for ca. 5 min before curing the monomer mixture under UV for 5 min (Dymax 5000-EC Series UV flood exposure lamp, nominal power 225 mW/cm^2, Dymax Corporation, Torrington, CT). After curing, the OSTE-

based micropillar array was sealed by laminating a planar cover layer of the same composition, prepared in the same manner, on top of the micropillar array, and finalized by an additional UV exposure for 2 min (Dymax 5000-EC). The biotinylation of the micropillar array was achieved by filling the microchannel with 0.1 mg/mL biotin-PEG_4-alkyne (Sigma Aldrich) in ethylene glycol, with 1% (m/v) Irgacure® TPO-L (BASF, Ludwigshafen, Germany) as the photoinitiator, after which the cross-linking reactions between biotin-PEG_4-the alkyne and the surface thiols were initiated by UV (LED, λ = 365 nm, nominal intensity 14 mW/cm^2). After UV exposure (1 min), the microchannel was rinsed sequentially with methanol (Sigma Aldrich) and Milli-Q water (3-5 mL each) and dried before use. The structural fidelity of the micropillar arrays was confirmed by scanning electron microscopy (Quanta™ 250 FEG, FEI, Hillsboro, OR) using a platinum coating (ca. 10 nm coating thickness).

Before loading the biotinylated pan-HLA antibody (1.6 mg/mL in PBS, BioLegend), the biotin-functionalized micropillars were precoated by filling the micropillar array with streptavidin (0.1 mg/mL in PBS, Sigma Aldrich), incubating for 15 min, and rinsing with 200uL of PBS three times.

Whenever fluorescent labelled streptavidin or antibodies were used, the quantitation of the fluorescence signal arising from on-chip immobilized biomolecules was performed through the top layer of the chip using a Zeiss Axioscope A1 upright epifluorescence microscope (Carl Zeiss Oy, Espoo, Finland) equipped with a HAL100W broadband lamp (Carl Zeiss) and a Hamamatsu R5929 photomultiplier tube coupled with a Cairn Integra signal amplifier module (Cairn Research, Faversham, UK). The on-chip fluorescence signals (excitation 488±5 nm, emission 500-700 nm) were quantitated and averaged from total of 3 locations along the micropillar array. Typically, 3-4 technical replicates (chips) were used.

Bioinformatic analysis

The functional annotation and visualisation was performed by using the clusterProfiler (19) Bioconductor package (v. 3.12.0) in the RStudio server environment (v. 3.6.0). ClusterProfiler implements a hypergeometric test to evaluate the statistical enrichment of the input gene list over the desired functional classes. Nominal p-values were adjusted by applying the Benjamini-Hochberg method (20) and the threshold was set to padj=0.01. The mapping between different human gene identifiers was performed through the use of the org.Hs.eg.db Bioconductor library (21) . The analysis of the Molecular Signatures Database (MSigDB) [URL: https://www.gsea-msigdb.org/gsea/msigdb] was performed by using the msigdbr CRAN package, while the visualisation of the results was obtained by employing the ComplexHeatmap Bioconductor package (22).

Statistical analyses

Statistical analysis was performed using GraphPad Prism 8.0 software (GraphPad Software Inc.). Details about the statistical tests for each experiment can be found in the corresponding figure legends.

Results

Customized microfluidic pillar arrays represent a novel and reliable approach for antibody immobilization in antigen discovery applications

We envisioned that all the immune-purification steps could be carried out within a single microfluidic chip by adding a biotinylated pan-HLA antibody to a streptavidin-prefunctionalized solid support structure (i.e., the micropillar array) and eventually immobilizing the HLA onto the pan-HLA antibody coated solid surface. The protocol was translated to microchip-scale to be able to address the diverse limitations posed by the current state-of-the-art methodologies (e.g., limited availability of samples, expensive consumable materials including monoclonal antibody). First, OSTE polymer based micropillar arrays were fabricated by a UV-replicamolding technique and biotinylated. Next, the biotinylated micropillars were functionalized with streptavidin and the biotinylated pan-HLA antibody was added, after which the cell lysate was loaded directly into the microfluidic chip to selectively trap the HLA-I complexes. After adequate washing, the trapped HLA-I complexes were eluted at room temperature by applying 7% acetic acid (**Fig. 1**). Thereafter, the protocol proceeded according to the standard immunopeptidomics workflow, including purification of the eluted HLA peptides with SepPac-C18 in acetonitrile and evaporating them to dryness by using vacuum centrifugation.

To investigate the robustness of the microchip technology, the selectivity of each step of the microchip functionalization protocol was examined. The efficiency of the streptavidin functionalization on pre-biotinylated micropillar arrays was examined with respect to two different incubation times (15 min and 1 h), with the help of fluorescent AlexaFluor488-streptavidin. The shorter incubation time was found sufficiently long for building the first streptavidin layer (**Fig. 2A**). Moreover, to determine the effect of the streptavidin concentration on the final amount of immobilized biotinylated pan-HLA antibody, several concentrations of non-fluorescent streptavidin were tested in the presence of a fixed amount of the biotinylated pan-HLA antibody. In this case, the biotinylated pan-HLA antibody was incubated for 15 min followed by three washing steps with PBS (200 µl for each step). To quantitate the amount of the immobilized biotinylated pan-HLA antibody at each streptavidin concentration, a fluorescent-labelled AlexaFluor488 secondary antibody was used to titer the immobilized biotinylated pan-HLA antibody. Interestingly, even a 10-fold increase in the streptavidin concentration did not much affect the amount of immobilized biotinylated pan-HLA antibody (**Fig. 2B**), which likely resulted from steric hindrances limiting the number of available streptavidin binding sites. On the basis of this finding, no further concentrations of streptavidin were explored, but the highest streptavidin concentration tested (0.1 mg/mL) was used in all subsequent experiments to ensure maximal binding of the biotinylated pan-HLA antibody. However, to further investigate the selectivity of the antibody binding onto the streptavidin functionalized micropillar surface, the impact of an additional coating step with bovine serum albumin (BSA) on the amount of immobilized biotinylated pan-HLA antibody was examined with a view to eliminate nonspecific interactions. To this end, the micropillar array was preconditioned with BSA (100 mg/mL in 15mM PBS, 10 min incubation) after streptavidin functionalization and the efficiency of subsequent binding of the biotinylated pan-HLA antibody was again determined with the help of the fluorescent-labelled secondary antibody. This procedure substantially reduced the amount of immobilized pan-HLA antibody in comparison to the non-preconditioned surfaces (**Fig. 2C**) suggesting that nonspecific binding sites could

be blocked with a simple BSA preincubation step. Therefore, the BSA incubation step was adapted for all futher experiments.

Finally, we sought to characterize the maximum amount of immobilized biotinylated pan-HLA antibody that can be bound onto a single chip by using the optimized protocol. This was evaluated through the use of multiple loading cycles of a new antibody batch of the same concentration (0.5 mg/mL) per a single microfluidic chip. In this case, the amount of the immobilized pan-HLA antibody was determined by comparing the pan-HLA antibody amount in the feed solution versus the output solution through an ELISA assay. It was observed that the amount of immobilized antibody increased almost linearly along with the number of loading cycles (**Fig. 2D**), allowing an accurate adjustment of the total amount of immobilized biotinylated pan-HLA antibody based on the number of loading cycles. After seven cycles, the amount of immobilized antibody reached the approximate amount of 45 µg, which suffices, at least theoretically, for the immunopeptidome investigation of scarce biological material as 10 mg of the pan-HLA ($5.6x10^{26}$ molecules of antibody) is required by the state-of-the-art methodologies for the investigation of 10^9 number of cells (22) (**Table 1**).

With the microchip setup, $4.2x10^{24}$ molecules of antibody could be immobilized and technically $7.5x10^6$ cells could be investigated.

Taken together, these results clearly demonstrate the feasibility of the chip-based protocol for immobilizing the pan-HLA antibody, via quick biotin-streptavidin chemistry, which further paves the way for a novel immunopetidomics workflow enabling identification of the HLA peptides from substantially lower sample amounts compared with the current state-of-the-art protocols.

Microchip-based antigen enrichment implemented in the immunopeptidomics workflow allows the identification of naturally presented HLA-I peptides

To assess whether the developed thiol-ene microchip could be exploited as an IP platform for antigen discovery applications, we immunopurified HLA peptides from the human B-cell lymphoblastoid cell line JY. The JY line has high expression of class I HLA and is homozygous for three alleles common in the human population (HLA-A*02:01, HLA-B*07:02 and HLA-C*07:02) (23) (**Supp. Fig. 1A-B**), and it has been extensively adopted for ligandome analysis, generating several publicly available ligandome repertoires (3). Consequently, the JY cell line was considered a suitable model for benchmarking the microchip-based IP technology.

Hence, HLA-I complexes were immunoaffinity-purified using the thiol-ene microchips, functionalized with the amount of pan-HLA antibody as described above. Moreover, to determine the sensitivity of our approach, the protocol was challenged by using total cell numbers as low as $50x10^6$, $10x10^6$ and $1x10^6$. The lysates were loaded into the microchips, and after adequate washing with PBS, the peptides were eluted with 7% acetic acid and analysed by tandem mass spectrometry. The entire workflow took an average from the streptavidin functionalization to the elution of the tumour peptides of <24 hours. A stringent false discovery rate threshold of 1% for peptide and protein identification was applied to

generate data with high confidence. We were able to identify 5589, 2100 and 1804 unique peptides from $50x10^6$, $10x10^6$ and $1x10^6$ cells, respectively (duplicates for each condition) (**Fig. 3A**).

As we sought to carefully analyse the ability of the microchip technology to enrich for natural HLA-I binders and to avoid potential coeluting contaminants, we extensively characterized the eluted peptides. First, the eluted peptides from JY cell line represented the typical length distribution of a ligandome data set, with 9mers as the most enriched peptide species (**Fig. 3B-E**). Next, the predicted binding affinity for the two HLA-I alleles (HLA-A*0201 and HLA-B*0702) expressed in JY cells was determined. JY cells also have a low level of the allele HLA-C*0702, but the binding motif overlaps with the motifs of HLA-A*0201 and HLA-B*0702; hence, only these alleles were considered in the subsequent analysis (3).

Of the unique 9mers, 78%, 83% and 67% were predicted to be binders (described as binders in NetMHCpan4.0, applied rank 2% (24-26)) to either HLA-A*0201 or HLA-B*0702 alleles for $50x10^6$, $10x10^6$ and $1x10^6$ cells, respectively (**Fig. 4A**). Moreover, Gibbs analysis was performed to deconvolute the consensus binding motifs of respective HLA-I alleles from the eluted 9mer peptides; these clustered in two distinct groups, with a preference for reduced amino acid complexity for residues at positions P2 and W, matching remarkably well with the known ones for HLA-A*0201 and HLA-B*0702 (**Fig. 4B**).

Next, in order to determine the role of the peptides identified, a gene ontology (GO) term enrichment analysis was performed on our list of 9mer binder source proteins. We observed an enrichment in nuclear and intracellular proteins, mainly those interacting with DNA, RNA or involved in catabolic activity (**Fig. 5A**) (**Suppl. Fig. 2**). These findings were in line with reports derived from other data sets (27-29). Intriguingly, the Molecular Signature Database (MSigDB) analysis reflected immune-associated and intracellular pathways important for B-cell biology. Indeed, we found proteins involved in IL-6 signalling (required for B-cell maturation), PI3K signalling in B lymphocytes (crucial in B-cell development), JAK2 in cytokine signalling (very active in stimulated B cells), and TGF-b signalling (regulator of B cell development and function) (30, 31) (**Fig. 5B**) (**Suppl. Fig. 3**). Finally, we set up an *in vitro* killing assay to further demonstrate the capacity of the microchip technology in isolating peptides in complex with HLA-I. To this end, a set of three peptides was selected from our JY data set to stimulate HLA-matched PBMCs; CD8+ T cells were purified from the PBMCs and adopted as effector cells in coculture with JY cells. To account for nonspecific cytotoxicity due to the effector cells *per se*, unstimulated PBMCs were used as a control. Real time cytolysis was then monitored. Interestingly, the CD8+ T cells pulsed with the peptides QLVDIIEKV (gene name PSME3) and KVLEYVIKV (gene name MAGEA1) showed ~10% specific cytolysis, whereas the CD8+ T cells pulsed with the peptide ILDKKVEKV (gene name HSP90AB3P) induced 15% specific cytolysis (**Fig. 5C**), indicating specific lysis in the presence of defined peptides.

To evaluate the validity of our HLA-I peptide lists identified by the microchip technology, we interrogated SysteMHC, a repository of the immunopetidomics data set generated by mass spectrometry. Among the unique 9mer binders identified in our data, 69%, 77% and 81% were also found in a previously published ligandome data set derived from the JY cell line (pride ID PXD000394) (3) for $50x10^6$, $10x10^6$ and $1x10^6$ cells, respectively (**Fig. 6A**). In addition, a positive correlation between the abundance of the source

protein and HLA presentation has been previously reported (3). Here, we sought to determine whether the same tendency was confirmed in our data sets. To this end, previously published JY proteomics data (3) were used to retrieve the log_2 intensity of the source proteins present in our data sets. The analysis confirmed the previous assumption, with the most abundant proteins being the main source of the HLA peptides (**Fig. 6B).**

Furthermore, six peptides have recently been reported as natural HLA-I peptides from JY cells and have been used by Ghosh et al. (33) to validate immunopeptidomic assays suitable for pharmaceutical therapies. In line with this previous observation, some of these peptides were also found in our data sets from $50x10^6$ cells (three peptides), $10x10^6$ cells (four peptides) and $1x10^6$ cells (three peptides) (**Table 2**).

Hence, these results demonstrated that the chip-based protocol can be exploited as a reliable IP platform within the immunopeptidomic workflow, providing a valid alternative to the current state-of-the-art technology.

The novel microfluidic chip-based platform investigates the immunopeptidome profile in scarce tumour biopsy tissue.

As we demonstrated that the microchip-based technology can be exploited for the ligandome analysis of the model cell line JY, we aimed to challenge the platform for the investigation of a scarce tumour biopsy. Thus, an ovarian metastatic tumour (high grade serous) was collected from the patient and four pieces were derived from the tumoral border (S1, S2, S3 and S4); the central part of the tumour was collected as well (S5). Next, the samples were weighted and as summarized in **Fig. 7A**, the size averaged from a 0.01g to 0.06g. After the sample digestion, the obtained single cells suspension was lysed and processed through the microchip. Applying a stringent false discovery rate threshold of 1% for peptide and protein identification, 916, 695,172, 1128 and 256 unique peptides were identified respectively in S1, S2, S3, S4 and S5 (**Fig. 7A**). In line with a typical ligandome profile, a general enrichment (above 70%) was observed in 7-13mers specimens (**Fig.7A**). As regard absolute number and percentage, the aminoacidic length distribution showed that the 9mers specimens were the most representative (**Fig.7B**), confirming our and other previous immunopeptidomic analysis. Next, we further investigated the source proteins found in our data, applying Gene Ontology (GO) enrichment analysis. Consistently with a typical ligandome profile, metabolic processes were enriched in all the samples examined (**Suppl. Fig. 4A**). Additionally, the analysis revealed an increase in skin development pathway in line with the epithelial nature of the ovarian serous tumour here analyzed. Altogether, the results highlighted the feasibility of exploiting the developed microfluidic-chip platform to analyse scarce tumour biopsy.

The microchip-based protocol reveals the immunopeptidome landscape in patient-derived organoids

After demonstrating the feasibility of microchip-based IP technology for ligandome discovery, we sought to determine whether this technology could be applied to investigate the immunopeptidome landscape of scarce patient-derived clinical material. To this end, the microchip technology was challenged with as few as $6x10^6$ cells from patient-derived organoids (PDOs). We selected two patients from on-going precision

medicine study for urological cancers, a nephrectomy sample containing both benign and cancer tissue from clear cell renal cell carcinoma (ccRCC) patient and 1x1 cm sample from bladder cancer patient, which were further processed as 3D primary organoid cultures.

Applying the developed microchip technology and a stringent false discovery rate threshold of 1% for peptide and protein identification, we were able to identify a total of 576 and 2089 unique peptides in ccRCC and bladder PDOs respectively (duplicates for each PDO) (**Fig. 8A**). The number of retrieved peptides differed between the two samples, with bladder PDOs resulting in more peptides than ccRCC PDOs. It is well known that HLA expression influences the amount of isolated HLA-I peptides (22), and consistent with this, flow cytometry analysis revealed higher surface levels of HLA-A, HLA-B, and HLA-C in our bladder PDOs than in our ccRCC PDOs (**Suppl. Fig. 5A-B**), explaining the different yields of retrieved peptides from our samples. Analysis of the peptides showed a preference for 9- to 12mers (56.4% in ccRCC and 47.9% in bladder tumours) with an enrichment in the 9mer population, in line with the typical length distribution of ligandome analysis (33) (**Fig. 8B**). To discriminate between HLA-I binders and contaminants, Gibbs clustering and NetMHC4.0 analysis was performed. First, deconvolution of the 9mers showed that 55% and 67% in bladder and ccRCC PDOs, respectively, matched at least one of the patients' HLA alleles (**Suppl. Fig. 6A-B**). Next, NetMHC4.0 was applied to all 9mers identified in our data set. Among them, 46% and 69% were predicted to be binders of the specific HLA of the patients (**Suppl. Fig. 6C**). Next, the source proteins present in both our data sets were investigated. To this end, Gene Ontology (GO) enrichment analysis was performed. Consistent with our previous observations and published data sets (27-29), both samples showed an enrichment in intracellular and nuclear proteins interacting with RNA and involved in catabolic/metabolic processes. Interestingly, the analysis highlighted the enrichment of biological pathways crucial for neutrophil activity (**Fig. 9A**), confirming the immune-infiltrated nature of the tumour types (34).

To demonstrate that the microchip technology can be exploited for the rapid development of therapeutic cancer vaccines, we decided to set up a killing assay using PDOs as targets and PBMCs pulsed with the identified peptides as effector cells. As the amount of bladder PDOs was insufficient to proceed with further *in vitro* validation, we focused our analysis on ccRCC PDOs on the RNA level of the source proteins contained in our data set. We used transcriptomics levels to select putative tumour antigens using PBMC and healthy kidney tissue as reference sets (RNA data were retrieved from The Human Protein Atlas (35), and the first quartile of Log2 RNA was considered) (**Fig. 9B**) Next, PBMCs from healthy volunteers were pulsed with the selected peptides, and CD8+ T cells isolated from those cells were used in the assay. T cells pulsed with the peptide EVAQPGPSNR (gene name HSPG2) showed ~10% specific cytolysis (**Fig. 9C**); in contrast, the peptides VIMDALKSSY (gene name NNMT) and FLAEGGGVR (gene name FGA) were ineffective in eliciting specific CD8+ T cell responses. Interestingly, the pool of peptides (EVAQPGPSNR, VIMDALKSSY and FLAEGGGVR) reached a specific cytolysis of 15% (**Fig. 9C**) in our assay, overcoming the limits of the single peptide specific CD8+ T cells. Finally, we sought to investigate the recall T cells response in the ccRCC patient. To this end, unfractionated PBMCs derived from the patient were *in vitro* stimulated with the peptide EVAQPGPSNR whereas unstimulated PBMCs were

adopted as control. The derived CD8+T cells were then added to the ccRCC PDO showing an increased killing activity compared to the control group (**Fig. 9D**).

Overall, these data support the potential application of the developed microchip technology with limited clinical samples, overcoming the limitations encountered in ligandome discovery for tumour biopsies.

Discussion

The breakthrough of immune-checkpoint inhibitors (ICIs) targeting PD-1, PD-L1 and CTLA-4 and their clinical approval (36) have attracted increasing interest in the cancer immunotherapy field. Despite their clinical success, objective response rates are not yet satisfactory (20-30% for many types of cancer) (37), highlighting the need to combine ICI with approaches that aim to generate and sustain specific anti-tumour CD8+ T cells (*e.g.*, therapeutic cancer vaccines) (38, 39). In this scenario, to design effective tumour rejection and protection strategies, the reliable identification of tumour peptides binding to HLA-I has become a hot topic (6, 40, 41). The direct identification of the peptides from the HLA-I complex still represents the best-established and the most widely used method for their identification (42). Nevertheless, the immunopeptidomics workflow is relatively complex and thus represents a major bottleneck in the antigen discovery process (11). Currently, the inability to analyse immunopeptidomes from a small amount of biological materials (*e.g.*, tissue needle biopsy), the sample throughput, the cost and the affinity matrix adopted (which is both laborious and expensive to produce) in the current IP platform have been depicted as the main technical challenges to address (12). Indeed, the cross-linking method used to couple the affinity column with antibodies has been associated with loss of antibody during binding, increasing the cost due to heavy antibody consumption (13). Moreover, the Human Immuno-Peptidome Project (HIPP) meeting report indicated that during the purification steps, only approximately 0.5–3% of HLA peptides are recovered, with most peptides lost during IP (13, 14), making this procedure the major technology gap in the overall workflow (43).

It is clear that we need to develop new and more efficient strategies for the isolation of HLA-I peptides and that the field would greatly benefit from additional technical advancements (13).

In this work, we addressed several technical issues hindering the ligandome research, with main focus on the limited availability of material to analyse, on the cost of consumables and on prolonged protocols.

By exploiting the well-characterized biotin-streptavidin interaction to immobilize biotinylated pan-HLA antibody on streptavidin-functionalized surfaces, we were able to replace the current technology based on affinity matrices prepared via cross-linking reactions with a microchip platform. The limitations posed by the paucity of the material (*e.g.*, needle biopsy) inspired the work towards the implementation of a microfluidic protocol. In this work, we employed a custom microchip protocol involving a thiol-ene polymer-based micropillar array as the solid support for further biofunctionalization that enabled performing the entire IP procedure on a single microfluidic chip.

Thiol-enes are an emerging class of polymers that facilitate not only low-cost microfabrication via non-cleanroom replica moulding but also implementation of a wealth of subsequent, tailor-made surface functionalizations at a significantly low cost (44, 45). As our approach offers an unexplored tool for IP, the custom-designed protocol necessitated careful analysis of its specificity and robustness. Therefore, several characterization steps and thorough method validation were performed to establish the technical basis of the protocol.

First, every step of microchip surface functionalization was examined to set up the best experimental conditions for subsequent steps. By incorporating the microfabricated pillar architecture, the total surface area (A) to sample volume (V) ratio could be increased by about four-fold from ca. A/V=10.7 mm-1 for 'hollow' microchannels of the same size to ca. A/V=39.0 mm-1 to micropillar arrays. This was critical to increasing the binding capacity, while ensuring flawless filling of the chip thanks to the well-defined micropillar array. Instead of coating the microchip surface directly with the biotinylated pan-HLA antibody, we decided to build the first layer with streptavidin bound onto a pre-biotinylated (with biotin-PEG4-alkyne) microchip surface so as to get a longer linker out from the pillar surface, enhancing the antibody binding capacity. The effect of the streptavidin concentration was analysed in regard to its binding efficiency and then to the amount of immobilized antibody, which was shown to increase in a streptavidin concentration-dependent manner. However, even 10-fold increases in the tested concentrations showed only small differences, suggesting that the saturation of the antibody binding capacity was achieved. To further increase the selectivity of the interaction between streptavidin and the biotinylated pan-HLA antibody, we also included BSA incubation as the blocker step, after streptavidin coating, to avoid nonspecific antibody interaction that could interfere with the antibody activity. As expected, BSA preconditioning decreased the total amount of bound antibody, confirming that addition of BSA as the blocking agent reduces the nonspecific interaction of the antibody with the chip surface increasing the selectivity of the binding between streptavidin and biotinylated pan-HLA antibody. Using this functionalization protocol, the amount of pan-HLA antibody immobilized onto the chip was shown to increase somewhat linearly along with antibody loading cycles so that an antibody amount of 45 µg was reached after 7 cycles. This amount of pan-HLA antibody theoretically suffices for carrying out IP of scarce biological material, while being substantially lower than the amount employed in the current IP platform, which is typically between 1 and 10 mg of antibody (22). Next, we sought to investigate the feasibility of the microchip technology for incorporation as an integral component for IP in the ligandome protocol to investigate scarce biological material. On the basis of publicly available ligandome data and on the alleles profile (the cell line is homozygous for HLA-A*02:01, HLA-B*07:02 and HLA-C*07:02), the EBV-transformed human B-cell line JY appeared as a reliable model to evaluate whether the pan-HLA antibody functionalized microchip could serve as an IP platform in the ligandome analysis (23).

Hence, the validation of the microchip-based protocol was conducted by using the JY cell line and challenged with as few as $50x10^6$, $10x10^6$ and $1x10^6$ cells instead of the $5x10^8$-$1x10^9$ cells commonly required in the current state-of-the-art IP methodologies (22).

The peptides trapped by and eluted from the microchip clearly showed the typical length distribution of a ligandome data set, with an enrichment in 9mer species; moreover, NetMHC 4.0 analysis for HLA-A*02:01 and HLA-B*07:02, identified 78%, 83% and 67% of the 9mers as binders in the data set derived from $50x10^6$, $10X10^6$ and $1x10^6$ cells, respectively. The data were further corroborated by the deconvolution analysis (unsupervised Gibbs clustering) that identified motifs resembling the reference ones. We are aware that the JY cell line also expresses a low level of HLA-Cw* 07:02; however, the binding motifs overlap with the motifs of HLA-A*02:01 and HLA-B*07:02, hindering a reliable analysis for HLA-Cw*07:02, as reported in Bassani et al. (3). Accordingly, our analysis was focused on the HLA-A*02:01 and HLA-B*07:02 alleles. Following these first preliminary results, we further characterized the peptide list by GO and MSigDB analyses. These latter revealed an enrichment in nuclear and intracellular proteins, in line with published ligandome data sets (27-29); most importantly, an enrichment in pathways essential for B-cell biology was observed, consistent with the nature of the model used in the microchip methodology (EBV-transformed human B-cell line JY). Last, the validation of the identified peptides in an *in vitro* killing assay confirm that the peptides were actually presented on the JY cell surface, as they were killed in a specific CD8+ T cell-dependent fashion. The peptide ILDKKVEKV found in our data set elicited the higher percentage of specific cytolysis. This peptide is a known B cells epitope in the Immune Epitope Database (IEDB) and interestingly it derives from the pseudogene HSP90AB3P. In line with this, altered pseudogene expression in cancer has been reported (46). The upregulation of peptides derived from pseudogene could break the T cell tolerance, inducing the activation of autoreactive T cells(47). In this scenario, peptides from the pseudogene are interesting target to exploit for cancer therapeutic approaches. To benchmark our results with the state of the art in the ligandome field, we carefully compared our data with well-established and solid data sets. We investigated two main factors: the presence of our eluted 9mers in the reference database and the intensity of their source proteins; as a result, an average of 76% of the unique 9mers were also found in the reference database, and the abundance of the source proteins clearly showed a direct correlation with HLA presentation, consistent with previous observations (3). Moreover, the six peptides (AIVDKVPSV, SPQGRVMTI, RPSGPGPEL, YLLPAIVHI, KVLEYVIKV, and SPSSILSTL) recently listed as natural HLA-I peptides from the JY cell line in Ghosh et al. (33) were also present in our data sets. The comprehensive technical characterization and the method validation results derived from the microchip-based protocol in ligandome analysis of the model JY cell line clearly evidenced that the microchip protocol was a robust tool to be integrated with the immunopetidomics workflow and that the methodology could be exploited to investigate the antigen landscape of scarce clinically relevant material. This is a key aspect for applicability, since the primary target population, metastatic cancer patients, are rarely operated and therefore samples are mainly obtained by needle biopsies. The number of cells derived from a needle biopsy account from $1.65x10^6$ to $6x10^6$ with differences depending on the tumour models and medical personal expertise (48). In the clinical setting, the patient sample size often hinders HLA peptidome discovery, and several attempts in the field have been attempted in the field to tackle this limitation, for instance, by establishing cell lines or the use of patient-derived xenograft mouse models (18, 41). However, the manipulation of the patient-derived samples to obtain a sufficient amount of biomaterial is time- and cost-intensive, and additionally, it could compromise the biological significance. To assess whether the microchip technology could address these

issues at least in part, we applied the microchip technology for ligandome analysis of scarce ovarian tumour biopsies and then for the analysis of ccRCC and bladder tumour PDOs. The microchip-based technology was successfully exploited for the ligandome analysis of multiple scarce ovarian tumour biopsies, paving the way to the ligandome investigation of samples inaccessible to state-of-the-art methodologies in the field.

Recently, PDO cell pellets (biological replicate, $3.85x10^7$–$1x10^8$ cells/pellet) from colorectal cancer have been extensively investigated in immunopeptidomic analyses (49). In this work, we challenged the microchip technology by scaling down the amount of PDO cell pellets down to $6x10^6$ cells for each sample. As expected, the microchip was able to isolate peptides that resembled the typical ligandome length distribution. Additionally, the number of eluted peptides directly relied on the HLA surface level in the PDOs, confirming that the peptides were most likely HLA ligands. Of note, the biological pathway analysis of the source proteins strongly suggested tumour immune infiltration. Indeed, ccRCC exhibits recruitment of neutrophils that in turn support cell invasion by modulating the ERβ, VEGFa and HIF2α signalling pathways (34). Although bladder tissue under physiological conditions lacks neutrophil infiltration, tumoural transformation correlates with higher recruitment of neutrophils in the tumour site (50).

Last, we validated the eluted peptides from the ccRCC PDOs in an *in vitro* killing assay. Peptide selection is of utmost importance for T cell-based cancer immunotherapies, and several strategies have been pursued so far (43). In this work, we selected peptides based on the RNA expression level (data retrieved from Human Protein Atlas), prioritizing peptides that retained low expression in both healthy renal tissue and PBMCs as severe or lethal side effects due to the lack of tumour specificity have been reported in several cancer vaccine approaches (43). This strategy allowed the selection of three peptides to be employed for the stimulation of PBMCs from healthy donor. Interestingly, only CD8+ T cells isolated from PBMCs stimulated with the peptide EVAQPGPSNR elicited specific cytolysis. This peptide derives from the heparan sulfate proteoglycan (HSPG2) and has been reported as over-represented peptides HLA-I peptide in colorectal cancer (51), making it a tumour associated antigen to further investigate.

To the best of our knowledge, this work for the first time integrates chip microfluidic technologies as an effective component with the immunopeptidomics workflow, addressing the main issues that are universally recognized challenges in the field with regard to the scarcity of biological material, costs, long and laborious protocols and the need for extensive sample handling. Besides technical characterization and method validation, the microchip technology was adopted to the antigen discovery process of clinical samples (PDOs); among the reported results, the key finding was that our customized-designated microchip protocol was able to isolate HLA-relevant ligands from as few as $6x10^6$ cells instead of $3.85x10^7$–$1x10^8$ cells, which is the state of the art as recently reported in the same context (49).

We envision that this technology may be further developed for clinical practice in therapeutic cancer vaccine development.

Declarations

Acknowledgements

We thank all the participants for their support and advice. Moreover, flow cytometry analysis was performed at the HiLife Flow Cytometry Unit, University of Helsinki. The Electron Microscopy Unit of the Institute of Biotechnology, University of Helsinki, is acknowledged for providing access to the scanning electron microscope. This work has been supported by the European Research Council under the European Union's Horizon 2020 Framework programme (H2020)/ERC-CoG-2015 Grant Agreement No. 681219, the Helsinki Institute of Life Science (HiLIFE), the Jane and Aatos Erkko Foundation (decision 19072019), H2020 Rescuer Project, the Orion Research Foundation, the Jalmari and Rauha Ahokas Foundation, the Maud Kuistila Foundation, the Cancer Society of Finland (Syöpäjärjestöt), ERC (POC), Tekes, Business Finland and the Erling-Persson Family Foundation, Swedish Cancer Society, Swedish Childhood Cancer Society and Swedish Research Council. T.S. and S.T. acknowledge the Academy of Finland for personal funding (decisions 309608 and 314303).

Conflicts of Interest

Vincenzo Cerullo is a cofounder and shareholder at VALO Therapeutics. The other authors have no conflicts of interest.

References

1. Galon J, Bruni D. Approaches to treat immune hot, altered and cold tumours with combination immunotherapies. Nat Rev Drug Discov. 2019;18(3):197-218.
2. Melief CJ, van Hall T, Arens R, Ossendorp F, van der Burg SH. Therapeutic cancer vaccines. J Clin Invest. 2015;125(9):3401-12.
3. Bassani-Sternberg M, Pletscher-Frankild S, Jensen LJ, Mann M. Mass spectrometry of human leukocyte antigen class I peptidomes reveals strong effects of protein abundance and turnover on antigen presentation. Mol Cell Proteomics. 2015;14(3):658-73.
4. Singh-Jasuja H, Emmerich NP, Rammensee HG. The Tubingen approach: identification, selection, and validation of tumor-associated HLA peptides for cancer therapy. Cancer Immunol Immunother. 2004;53(3):187-95.
5. Dutoit V, Herold-Mende C, Hilf N, Schoor O, Beckhove P, Bucher J, et al. Exploiting the glioblastoma peptidome to discover novel tumour-associated antigens for immunotherapy. Brain. 2012;135(Pt 4):1042-54.
6. Berlin C, Kowalewski DJ, Schuster H, Mirza N, Walz S, Handel M, et al. Mapping the HLA ligandome landscape of acute myeloid leukemia: a targeted approach toward peptide-based immunotherapy. Leukemia. 2016;30(4):1003-4.

7. Walz S, Stickel JS, Kowalewski DJ, Schuster H, Weisel K, Backert L, et al. The antigenic landscape of multiple myeloma: mass spectrometry (re)defines targets for T-cell-based immunotherapy. Blood. 2015;126(10):1203-13.
8. Bassani-Sternberg M, Barnea E, Beer I, Avivi I, Katz T, Admon A. Soluble plasma HLA peptidome as a potential source for cancer biomarkers. Proc Natl Acad Sci U S A. 2010;107(44):18769-76.
9. Mommen GP, Frese CK, Meiring HD, van Gaans-van den Brink J, de Jong AP, van Els CA, et al. Expanding the detectable HLA peptide repertoire using electron-transfer/higher-energy collision dissociation (EThcD). Proc Natl Acad Sci U S A. 2014;111(12):4507-12.
10. Fritsche J, Rakitsch B, Hoffgaard F, Romer M, Schuster H, Kowalewski DJ, et al. Translating Immunopeptidomics to Immunotherapy-Decision-Making for Patient and Personalized Target Selection. Proteomics. 2018;18(12):e1700284.
11. Chong C, Marino F, Pak H, Racle J, Daniel RT, Muller M, et al. High-throughput and Sensitive Immunopeptidomics Platform Reveals Profound Interferongamma-Mediated Remodeling of the Human Leukocyte Antigen (HLA) Ligandome. Mol Cell Proteomics. 2018;17(3):533-48.
12. Caron E, Aebersold R, Banaei-Esfahani A, Chong C, Bassani-Sternberg M. A Case for a Human Immuno-Peptidome Project Consortium. Immunity. 2017;47(2):203-8.
13. Caron E, Kowalewski DJ, Chiek Koh C, Sturm T, Schuster H, Aebersold R. Analysis of Major Histocompatibility Complex (MHC) Immunopeptidomes Using Mass Spectrometry. Mol Cell Proteomics. 2015;14(12):3105-17.
14. Hassan C, Kester MG, Oudgenoeg G, de Ru AH, Janssen GM, Drijfhout JW, et al. Accurate quantitation of MHC-bound peptides by application of isotopically labeled peptide MHC complexes. J Proteomics. 2014;109:240-4.
15. Lee SH, Hu W, Matulay JT, Silva MV, Owczarek TB, Kim K, et al. Tumor Evolution and Drug Response in Patient-Derived Organoid Models of Bladder Cancer. Cell. 2018;173(2):515-28 e17.
16. Bassani-Sternberg M. Mass Spectrometry Based Immunopeptidomics for the Discovery of Cancer Neoantigens. Methods Mol Biol. 2018;1719:209-21.
17. Tahka S, Sarfraz J, Urvas L, Provenzani R, Wiedmer SK, Peltonen J, et al. Immobilization of proteolytic enzymes on replica-molded thiol-ene micropillar reactors via thiol-gold interaction. Anal Bioanal Chem. 2019;411(11):2339-49.
18. Yu G, Wang LG, Han Y, He QY. clusterProfiler: an R package for comparing biological themes among gene clusters. OMICS. 2012;16(5):284-7.
19. Benjamini Y, Hochberg Y. Controlling the False Discovery Rate: A Practical and Powerful Approach to Multiple Testing. Journal of the Royal Statistical Society Series B (Methodological). 1995;57(1):289-300.
20. M C. Genome wide annotation for Human. 2019.
21. Gu Z, Eils R, Schlesner M. Complex heatmaps reveal patterns and correlations in multidimensional genomic data. Bioinformatics. 2016;32(18):2847-9.

22. Purcell AW, Ramarathinam SH, Ternette N. Mass spectrometry-based identification of MHC-bound peptides for immunopeptidomics. Nat Protoc. 2019;14(6):1687-707.
23. Heather JM, Myers PT, Shi F, Aziz-Zanjani MO, Mahoney KE, Perez M, et al. Murine xenograft bioreactors for human immunopeptidome discovery. Sci Rep. 2019;9(1):18558.
24. Jurtz V, Paul S, Andreatta M, Marcatili P, Peters B, Nielsen M. NetMHCpan-4.0: Improved Peptide-MHC Class I Interaction Predictions Integrating Eluted Ligand and Peptide Binding Affinity Data. J Immunol. 2017;199(9):3360-8.
25. Nielsen M, Andreatta M. NetMHCpan-3.0; improved prediction of binding to MHC class I molecules integrating information from multiple receptor and peptide length datasets. Genome Med. 2016;8(1):33.
26. Hoof I, Peters B, Sidney J, Pedersen LE, Sette A, Lund O, et al. NetMHCpan, a method for MHC class I binding prediction beyond humans. Immunogenetics. 2009;61(1):1-13.
27. Pearson H, Daouda T, Granados DP, Durette C, Bonneil E, Courcelles M, et al. MHC class I-associated peptides derive from selective regions of the human genome. J Clin Invest. 2016;126(12):4690-701.
28. Hickman HD, Luis AD, Buchli R, Few SR, Sathiamurthy M, VanGundy RS, et al. Toward a definition of self: proteomic evaluation of the class I peptide repertoire. J Immunol. 2004;172(5):2944-52.
29. Hoof I, van Baarle D, Hildebrand WH, Kesmir C. Proteome sampling by the HLA class I antigen processing pathway. PLoS Comput Biol. 2012;8(5):e1002517.
30. Tamayo E, Alvarez P, Merino R. TGFbeta Superfamily Members as Regulators of B Cell Development and Function-Implications for Autoimmunity. Int J Mol Sci. 2018;19(12).
31. Granados DP, Yahyaoui W, Laumont CM, Daouda T, Muratore-Schroeder TL, Cote C, et al. MHC I-associated peptides preferentially derive from transcripts bearing miRNA response elements. Blood. 2012;119(26):e181-91.
32. Ghosh M, Gauger M, Marcu A, Nelde A, Denk M, Schuster H, et al. Guidance document: validation of a high-performance liquid chromatography-tandem mass spectrometry immunopeptidomics assay for the identification of HLA class I ligands suitable for pharmaceutical therapies. Mol Cell Proteomics. 2020.
33. Bassani-Sternberg M, Braunlein E, Klar R, Engleitner T, Sinitcyn P, Audehm S, et al. Direct identification of clinically relevant neoepitopes presented on native human melanoma tissue by mass spectrometry. Nat Commun. 2016;7:13404.
34. Song W, Yeh CR, He D, Wang Y, Xie H, Pang ST, et al. Infiltrating neutrophils promote renal cell carcinoma progression via VEGFa/HIF2alpha and estrogen receptor beta signals. Oncotarget. 2015;6(22):19290-304.
35. Uhlen M, Fagerberg L, Hallstrom BM, Lindskog C, Oksvold P, Mardinoglu A, et al. Proteomics. Tissue-based map of the human proteome. Science. 2015;347(6220):1260419.
36. Havel JJ, Chowell D, Chan TA. The evolving landscape of biomarkers for checkpoint inhibitor immunotherapy. Nat Rev Cancer. 2019;19(3):133-50.

37. Emens LA, Ascierto PA, Darcy PK, Demaria S, Eggermont AMM, Redmond WL, et al. Cancer immunotherapy: Opportunities and challenges in the rapidly evolving clinical landscape. Eur J Cancer. 2017;81:116-29.
38. Feola S, Capasso C, Fusciello M, Martins B, Tahtinen S, Medeot M, et al. Oncolytic vaccines increase the response to PD-L1 blockade in immunogenic and poorly immunogenic tumors. Oncoimmunology. 2018;7(8):e1457596.
39. Seliger B. Combinatorial Approaches With Checkpoint Inhibitors to Enhance Anti-tumor Immunity. Front Immunol. 2019;10:999.
40. Brennick CA, George MM, Srivastava PK, Karandikar SH. Prediction of cancer neoepitopes needs new rules. Semin Immunol. 2020:101387.
41. Yewdell JW, Reits E, Neefjes J. Making sense of mass destruction: quantitating MHC class I antigen presentation. Nat Rev Immunol. 2003;3(12):952-61.
42. Gfeller D, Bassani-Sternberg M. Predicting Antigen Presentation-What Could We Learn From a Million Peptides? Front Immunol. 2018;9:1716.
43. Freudenmann LK, Marcu A, Stevanovic S. Mapping the tumour human leukocyte antigen (HLA) ligandome by mass spectrometry. Immunology. 2018;154(3):331-45.
44. Kiiski IMA, Pihlaja T, Urvas L, Witos J, Wiedmer SK, Jokinen VP, et al. Overcoming the Pitfalls of Cytochrome P450 Immobilization through the Use of Fusogenic Liposomes. Adv Biosyst. 2019;3(1).
45. Sticker D, Geczy R, Hafeli UO, Kutter JP. Thiol-Ene Based Polymers as Versatile Materials for Microfluidic Devices for Life Sciences Applications. ACS Appl Mater Interfaces. 2020;12(9):10080-95.
46. Poliseno L, Marranci A, Pandolfi PP. Pseudogenes in Human Cancer. Front Med (Lausanne). 2015;2:68.
47. Herberts CA, van Gaans-van den Brink J, van der Heeft E, van Wijk M, Hoekman J, Jaye A, et al. Autoreactivity against induced or upregulated abundant self-peptides in HLA-A*0201 following measles virus infection. Hum Immunol. 2003;64(1):44-55.
48. Mirjana Rajer MK. Quantitative analysis of fine needle aspiration biopsy samples. Radiol Oncol. 2005;39.
49. Newey A, Griffiths B, Michaux J, Pak HS, Stevenson BJ, Woolston A, et al. Immunopeptidomics of colorectal cancer organoids reveals a sparse HLA class I neoantigen landscape and no increase in neoantigens with interferon or MEK-inhibitor treatment. J Immunother Cancer. 2019;7(1):309.
50. Joseph M, Enting D. Immune Responses in Bladder Cancer-Role of Immune Cell Populations, Prognostic Factors and Therapeutic Implications. Front Oncol. 2019;9:1270.
51. Loffler MW, Kowalewski DJ, Backert L, Bernhardt J, Adam P, Schuster H, et al. Mapping the HLA Ligandome of Colorectal Cancer Reveals an Imprint of Malignant Cell Transformation. Cancer Res. 2018;78(16):4627-41.

Tables

Table 1 Comparative analysis between microchip-based IP technology and the standard procedure. The table reports the total amount of antibody coated into the microchip-based IP technology and the standard procedure; the amount of antibody molecules is calculated according to the following formula:

$$\frac{\text{mass in gram}}{\text{molar mass}} \times \text{Avogadro's number}$$

where mass in gram is the total antibody consumed; the molar mass is 155000 g/mol (IgG isotype); the Avogadro's number is 6.02×10^{23}.

	Total antibody consumed	#of antibody moles	#of antibody molecules	Total amount of cells to use
Standard procedure	10mg	1550	9.3×10^{26}	1×10^{9}
Microchip	45μg	7	4.2×10^{24}	7.5×10^{6}

Table 2 Naturally HLA-I peptides isolated in JY cell line validated immunopetidomic assay. The table depicts **on the left** the list of naturally HLA-I peptides used to validate immunopeptidomic assay suitable for pharmaceutical therapies; **on the right** the list of the peptides found in our data sets for 50×10^6, 10×10^6 and 1×10^6 cells are indicated as a check mark.

Naturally HLA-I peptides (Gosh et al.)	50×10^6	10×10^6	1×10^6
AIVDKVPSV		✓	✓
RPSGPGPEL	✓	✓	✓
YLLPAIVHI			
KVLEYVIKV	✓	✓	
SPSSILSTL			
SPQGRVMTI	✓	✓	✓

Figures

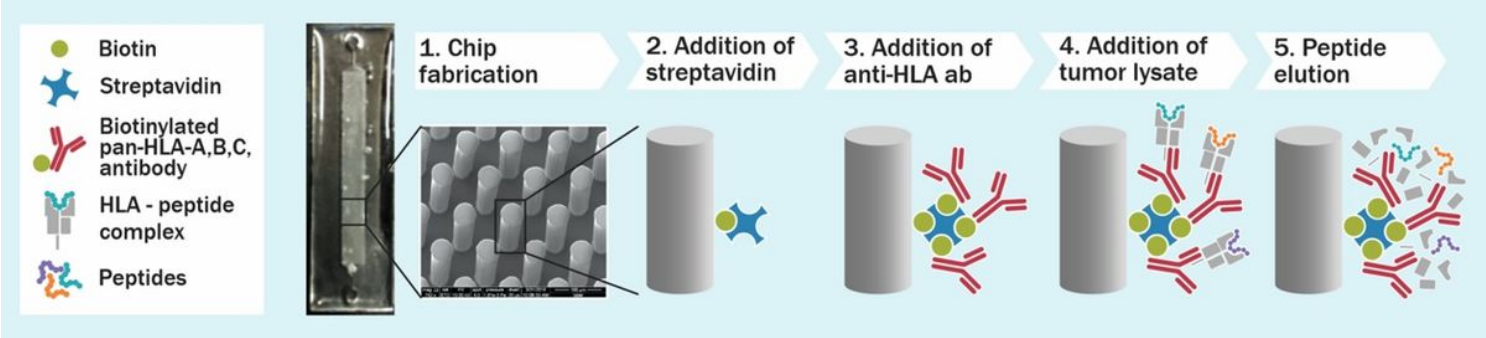

Figure 1

Microchip technology as a novel immunopurification platform for fast antigen discovery. A schematic overview describing the new microchip methodology developed. Thiol-ene microchips incorporating free surface thiols are derivatized with biotin-PEG4-alkyne thiolene (Step1) and functionalized with a layer of streptavidin (Step2) after which a biotinylated pan-HLA antibody is immobilized on the micropillar surface (Step3) and cell lysate is loaded into the microchip (Step4). After adequate incubation time and washing steps, the HLA molecules are eluted by adding 7% acetic acid (Step5).

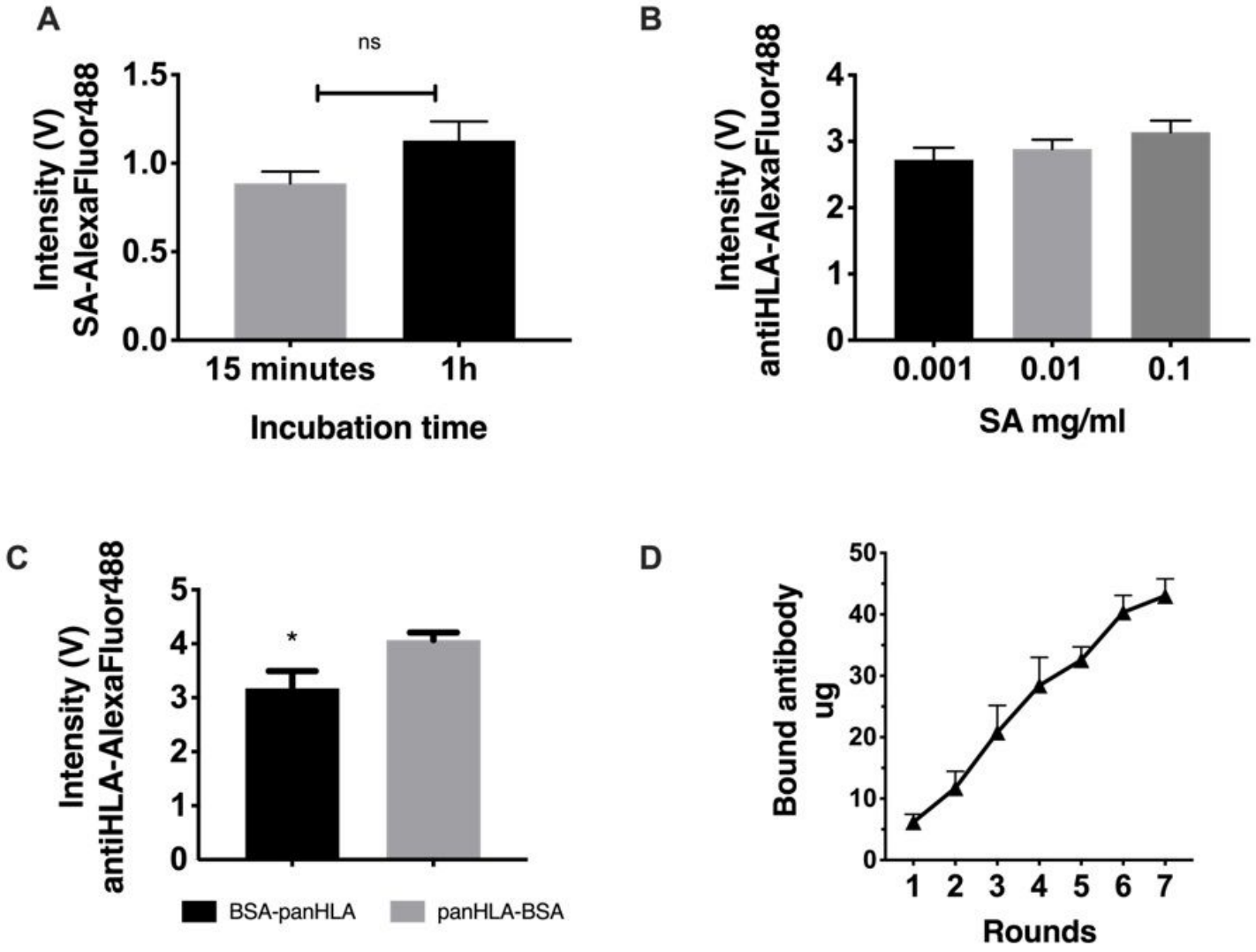

Figure 2

Characterization of the selectivity of the microchip functionalization with biotinylated pan-HLA antibody. A) Binding efficacy of AlexaFluor 488-streptavidin on thiol-ene micropillars precoated with biotin-PEG4-alkyne at two different streptavidin incubation times (15 min and 1h). B) The effect of streptavidin (nonfluorescent) concentration on the amount of immobilized biotinylated pan-HLA antibody quantitated through AlexaFluor 488-labeled secondary antibody. C) The effect of BSA incubation on the amount of immobilized biotinylated pan-HLA antibody quantitated through AlexaFluor 488-labeled secondary antibody. The efficiency of BSA in blocking nonspecific binding sites was assessed by preconditioning the micropillar array with BSA either before (BSA-panHLA) or after (panHLA-BSA) immobilization of the biotinylated pan-HLA antibody. D) The total amount of biotinylated pan-HLA antibody bound onto a single chip as a function of loading cycles. For each cycle, a fresh batch of the same (constant) pan-HLA antibody concentration was used. Significance was assessed by two-tailed unpaired Student's t-test, * $p<0.05$. All the technical characterization was performed at least two time in two separate experiment and in each experiment at least triplicates for each group was performed.

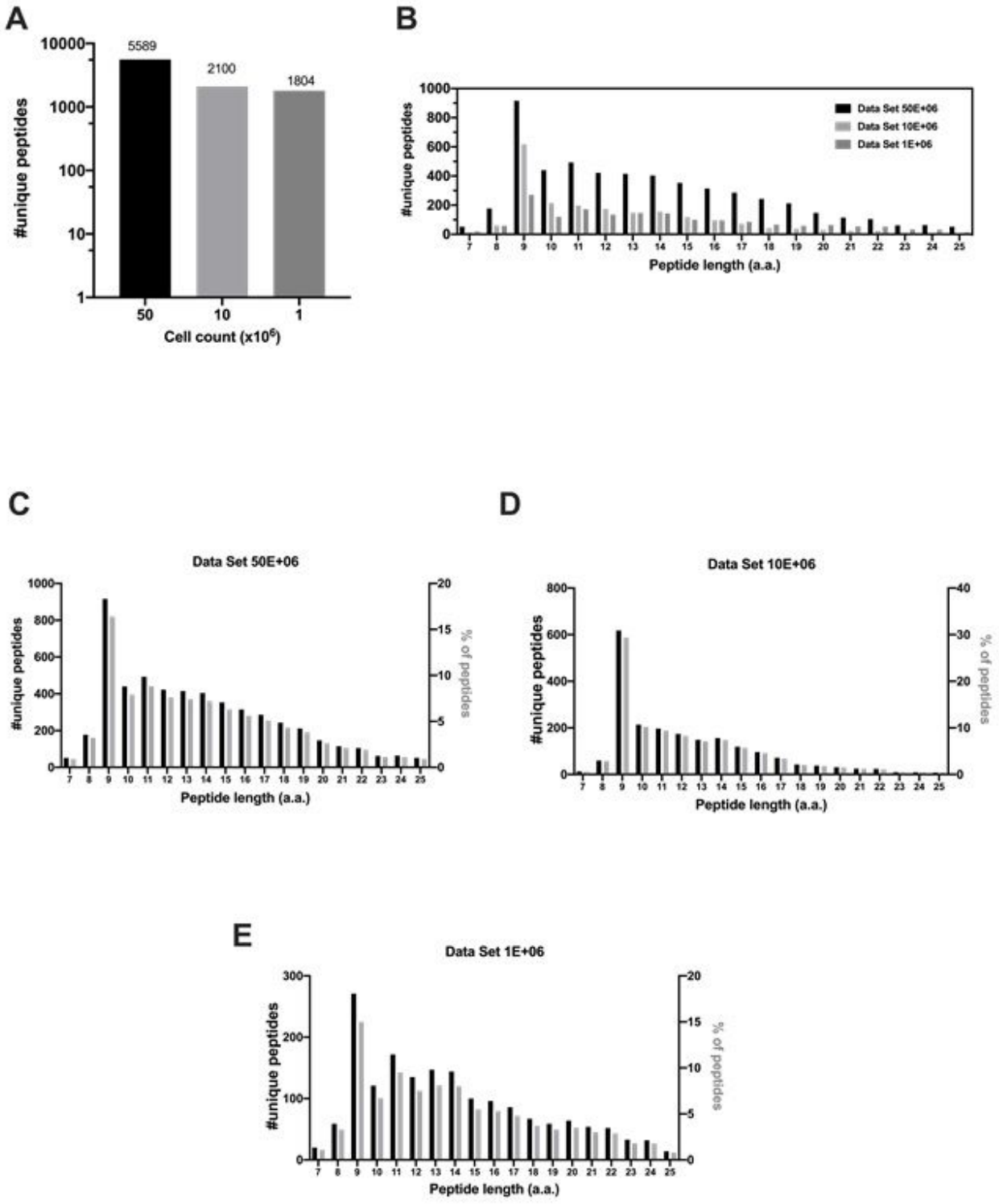

Figure 3

Properties of the HLA-I peptidomes data set obtained from JY cell line. A) Number of unique peptides eluted from 50x106, 10x106 and 1x106 JY cells. B) Overall peptide length distribution of the HLA peptides in the three data sets derived from the JY cell line C-E) Length distribution of HLA peptides is depicted as number of unique peptides (left y axis) and percentage of occurrence (right y axis) for 50x106 (C), 10x106 (D) and 1x106 (E).

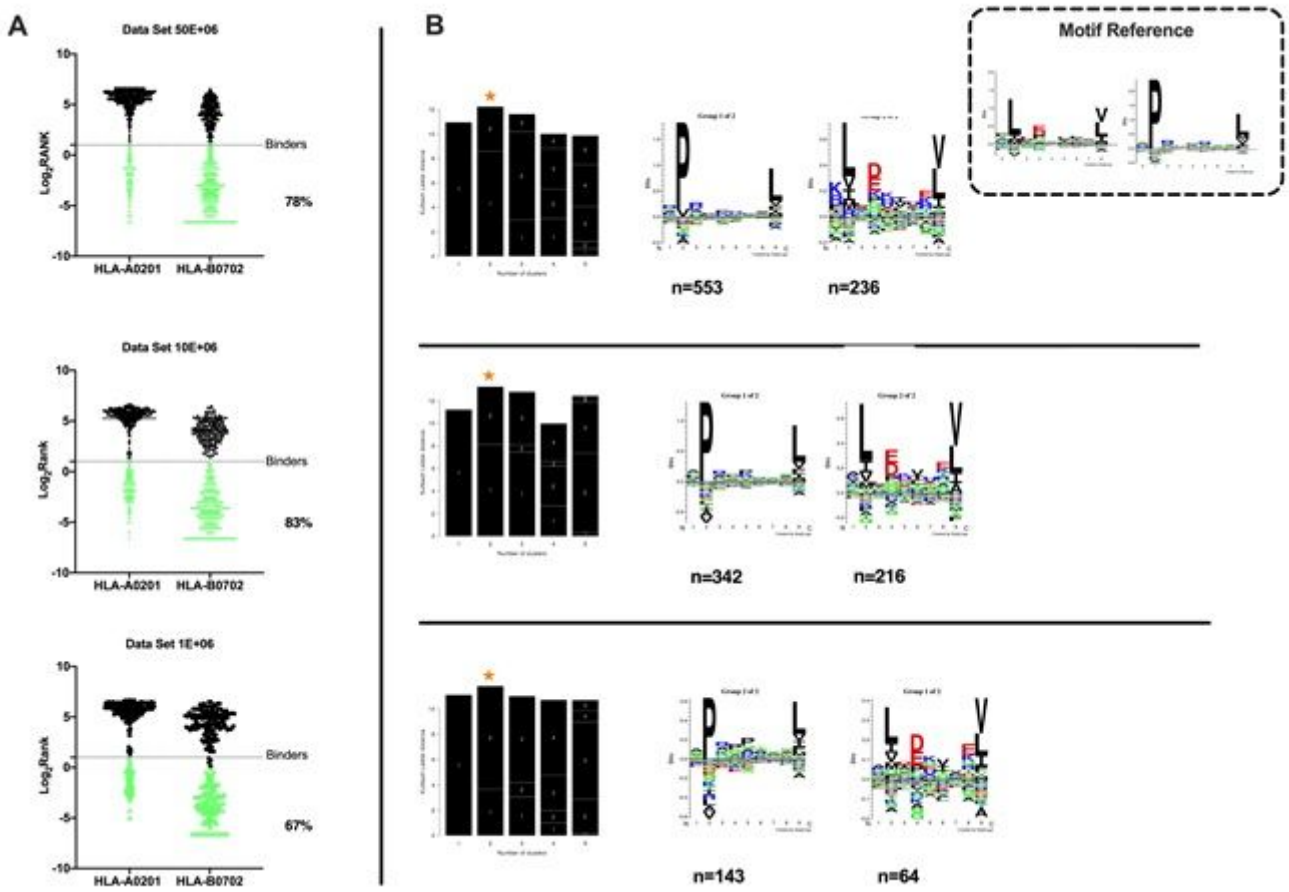

Figure 4

Accurate analysis of HLA ligands isolated from JY cell line. A) The eluted 9mers were analyzed as regard to their binding affinity to HLA-A*02:01 and HLA-B*07:02. The binders (green dots) and not binders (black dots) were defined in NetMHCpan 4.0 Server (applied rank 2%). B) HLA-I consensus binding motifs. Gibbs clustering analysis was performed to define the consensus binding motifs among the eluted 9mers peptides. The reference motif is depicted in the upper right corner. The clusters with the optimal fitness (higher KLD values, orange star) are showed and the sequence logo is represented with the number of HLA-I for each cluster.

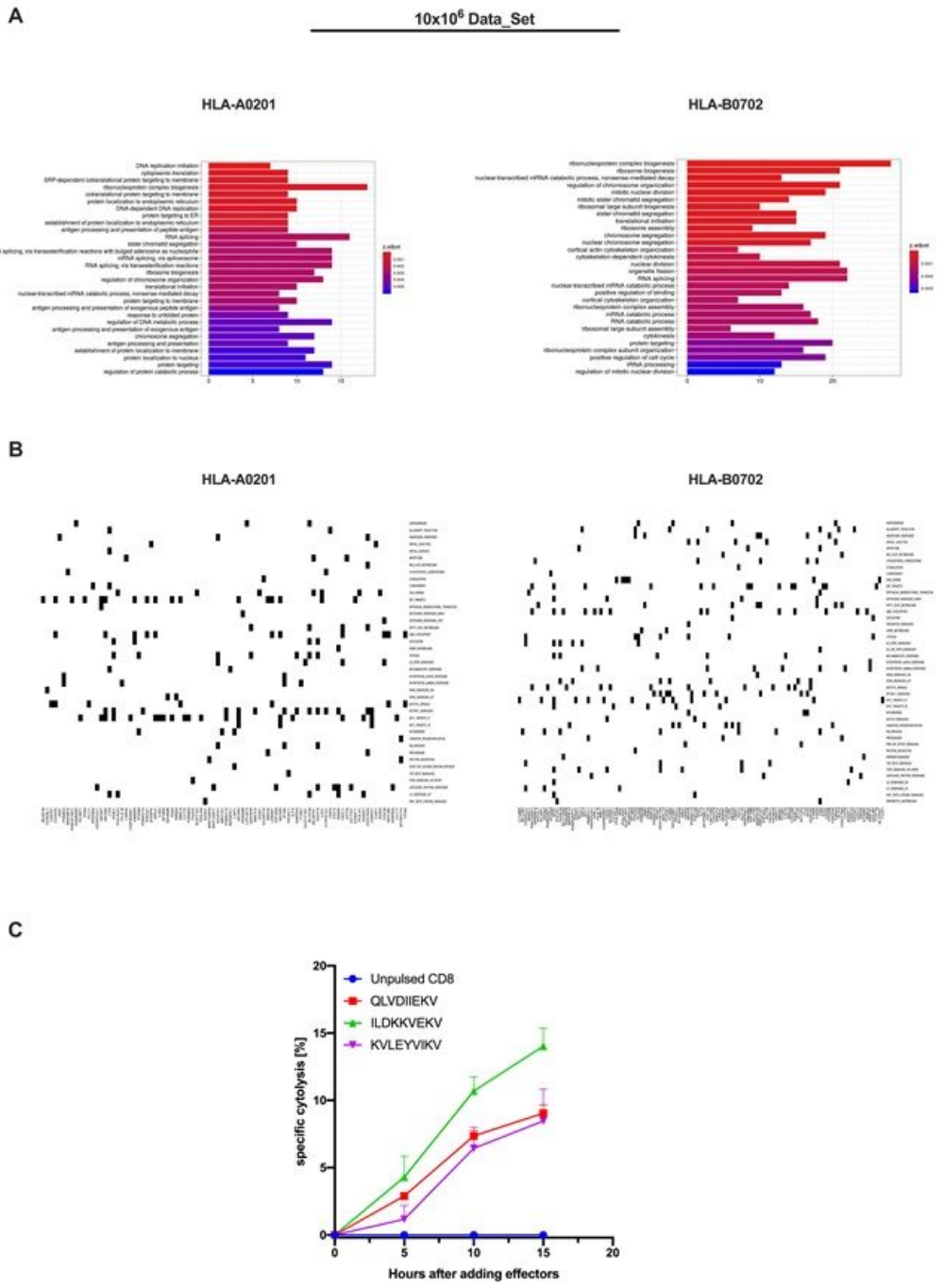

Figure 5

In depth enrichment analysis of HLA-ligands source proteins and CD8+ T-cell based cytotoxic assay. A) Gene ontology enrichment analysis of the HLA-ligands source proteins. The most overrepresented biological processes for 10x106 cells are separately shown for HLA-A*02:01 and HLA-B*07:02 alleles (hypergeometric test padj<0.01) B) Molecular Signature Database results are displayed. The source proteins analysis was performed against the hallmark data set and separately for HLA-A*02:01 and HLA-

B*07:02 alleles. C) PBMCs from healthy donors were pulsed for 9 days with the indicated peptides and at day 10 CD8+T cells were isolated and used in an in vitro killing assay at E:T 1:1. The time-response is showed after adding the effectors.

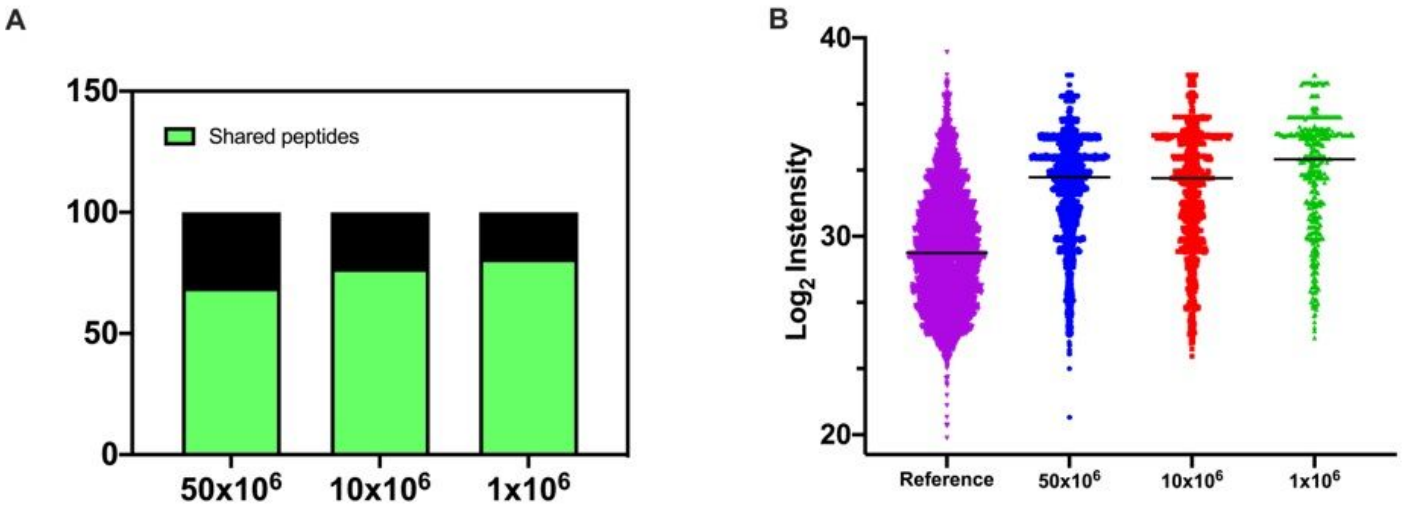

Figure 6

Comparative analysis of the generated datasets from JY cell line. A) The percentage of the shared 9mers has been calculated against a depository reference data set (pride ID PXD000394) derived from the JY cell line; the results are depicted as bar plot and the percentage of shared peptides is indicated in green. B) The abundance of the source proteins is expressed in Log2 Intensity and the values are derived from a reference published proteomic analysis of total JY cell lysate. The plot showed the comparison among the three data sets (50x106 cells, 10x106 cells and 1x106) generated through our microchip technology and the reference data set.

A

	S1	S2	S3	S4	S5
Weight	**0.06gr**	**0.05g**	**0.05g**	**0.01g**	**0.02g**
Total number of peptides	**935**	**715**	**172**	**1155**	**260**
Unique peptides (no duplicates peptides)	**916**	**695**	**172**	**1128**	**256**
7-13mers	**689 (75%)**	**580 (83%)**	**124 (72%)**	**924 (82%)**	**201 (79%)**

B

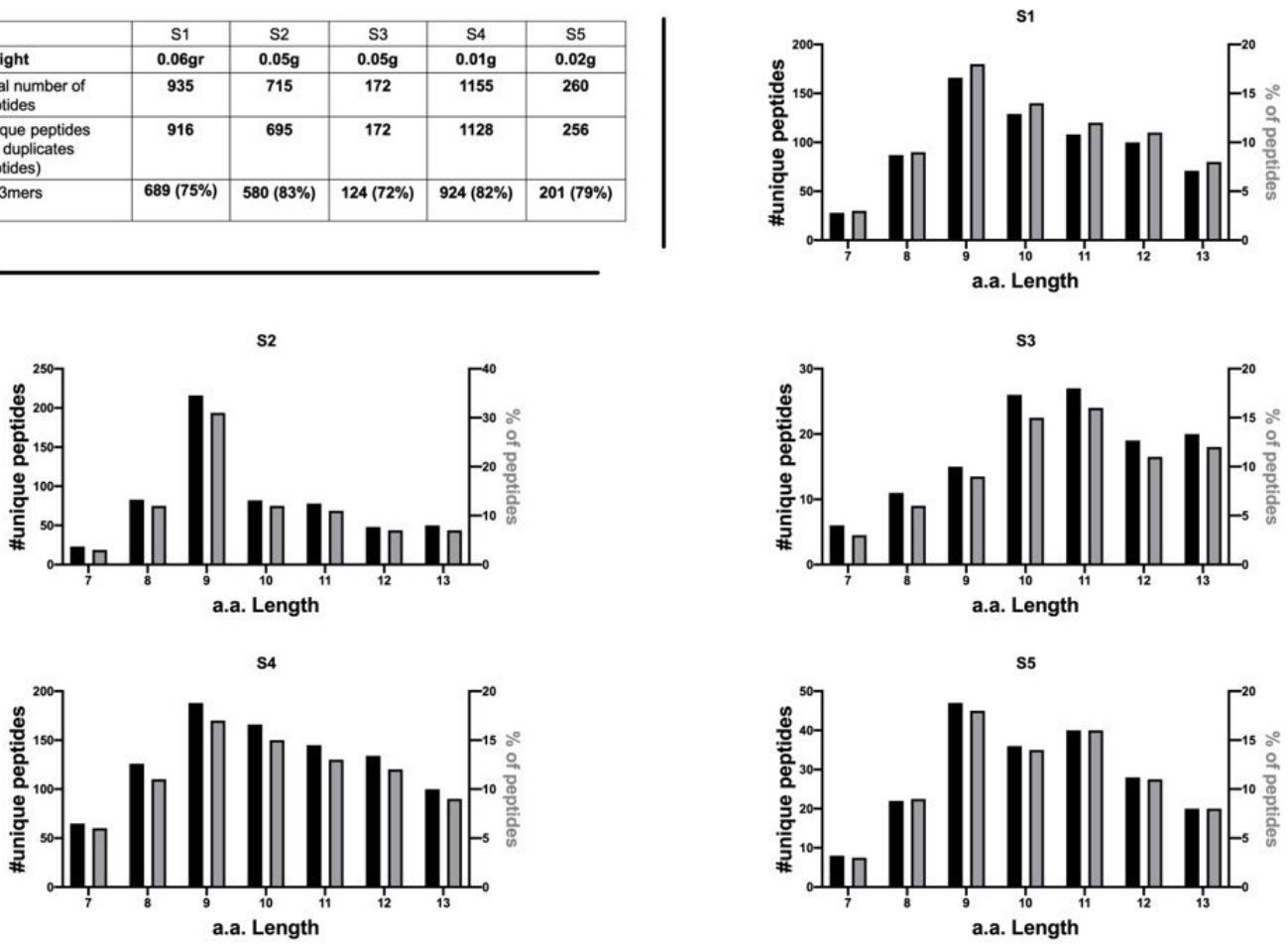

Figure 7

Microchip based platform reveals the immunopepetidomic profile in scarce tumour biopsies. A) The weight of the samples before the processing, the total number and the unique peptides and the enrichment in 7-13mers specimens are summarized here. B) The length distribution of the peptides as regard their absolute number and the percentage are showed as bars plot.

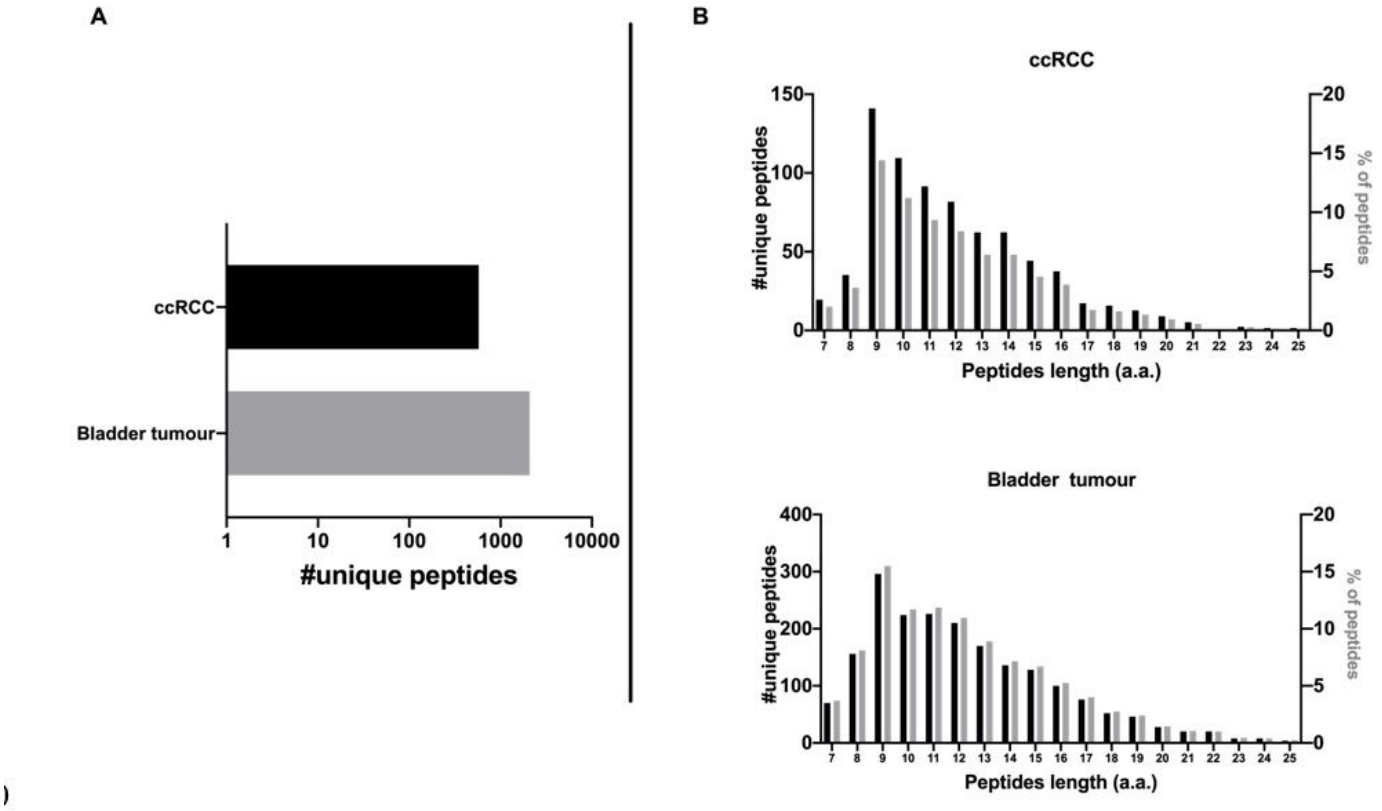

Figure 8

Immunopeptidomic analysis of ccRCC and Bladder tumour patient derived organoids (PDO). A) Number of unique peptides detected in ccRCC and Bladder PDOs. B) The peptides length distribution is showed as total number of unique peptides (left y axis) and percentage of occurrence (right y axis) per each PDO (ccRCC upper panel, bladder lower panel).

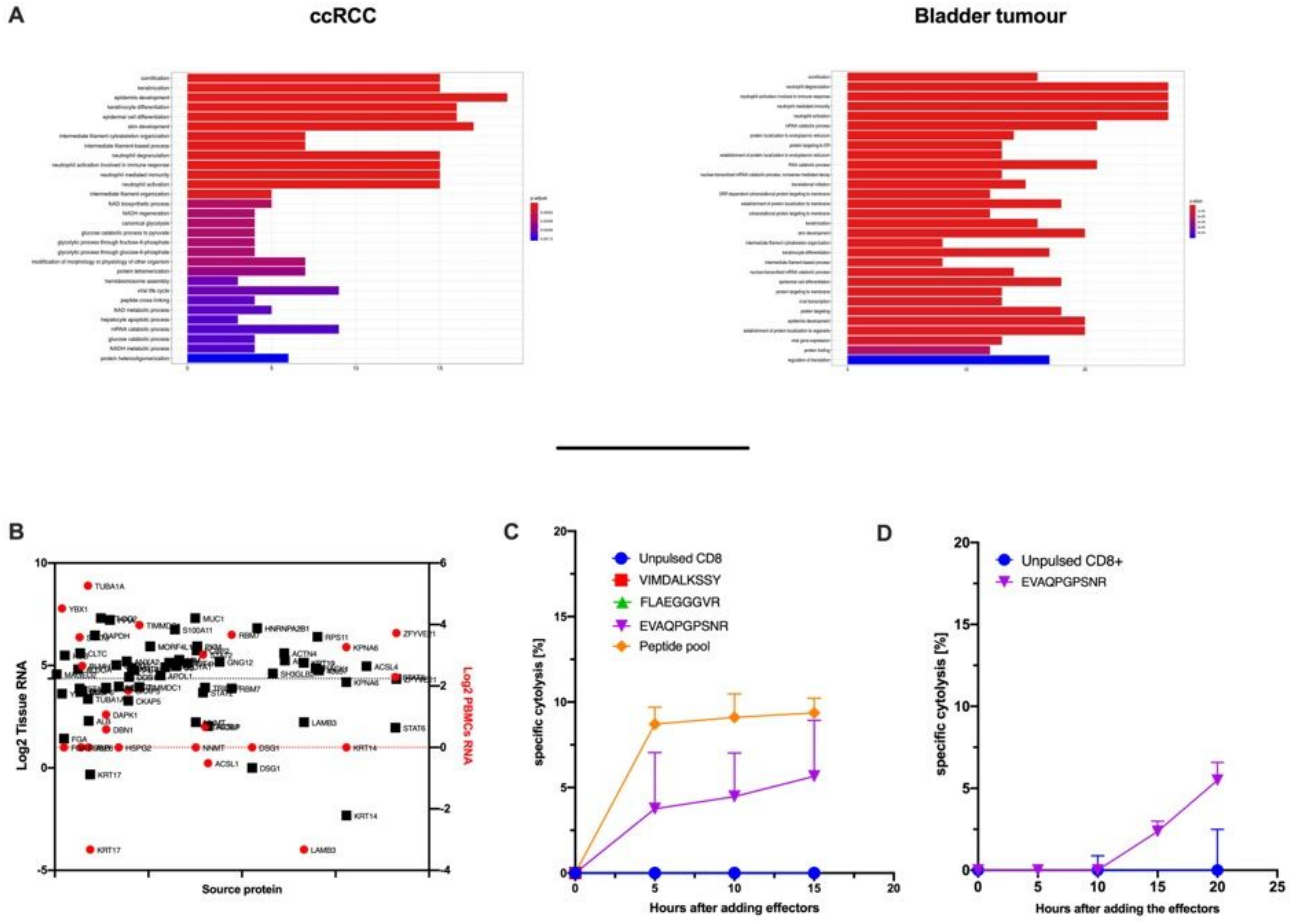

Figure 9

Assessment of the immunopeptidomic profile in PDOs. A) Gene ontology enrichment analysis. The most overrepresented biological processes for RCC (left panel) and Bladder (right panel) PDOs are shown (hypergeometric test padj<0.01) B) The source proteins expression is depicted as Log2 of the RNA level in healthy kidney tissue (black square) and in blood PBMCs (red circle). The 1st quartile is indicated as black and red dashed line respectively for the healthy kidney tissue and blood PBMCs. C) PBMCs from healthy donors or D) PBMCs from patients were pulsed for 9 days with the indicated peptides and at day 10 CD8+T cells were isolated and used in an in vitro killing assay at E:T 1:1. The time-response is showed after adding the effectors.

Supplementary Files

This is a list of supplementary files associated with this preprint. Click to download.

- SupplementaryFigures.pdf